Journal of Virology

The Tobacco mosaic virus Movement Protein Associates with but Does Not Integrate into Biological Membranes

Ana Peiró, Luis Martínez-Gil, Silvia Tamborero, Vicente Pallás, Jesús A. Sánchez-Navarro and Ismael Mingarro

***J. Virol.* 2014, 88(5):3016. DOI: 10.1128/JVI.03648-13.**
Published Ahead of Print 26 December 2013.

JVI Journals.ASM.org

The *Tobacco Mosaic Virus* Movement Protein Associates with but Does Not Integrate into Biological Membranes

Ana Peiró,[b] Luis Martínez-Gil,[a] Silvia Tamborero,[a] Vicente Pallás,[b] Jesús A. Sánchez-Navarro,[b] Ismael Mingarro[a]

Departament de Bioquímica i Biologia Molecular, Universitat de València, Burjassot, Spain[a]; Instituto de Biología Molecular y Celular de Plantas, Universidad Politécnica de Valencia–CSIC, Valencia, Spain[b]

ABSTRACT

Plant positive-strand RNA viruses require association with plant cell endomembranes for viral translation and replication, as well as for intra- and intercellular movement of the viral progeny. The membrane association and RNA binding of the *Tobacco mosaic virus* (TMV) movement protein (MP) are vital for orchestrating the macromolecular network required for virus movement. A previously proposed topological model suggests that TMV MP is an integral membrane protein with two putative α-helical transmembrane (TM) segments. Here we tested this model using an experimental system that measured the efficiency with which natural polypeptide segments were inserted into the ER membrane under conditions approximating the *in vivo* situation, as well as *in planta*. Our results demonstrated that the two hydrophobic regions (HRs) of TMV MP do not span biological membranes. We further found that mutations to alter the hydrophobicity of the first HR modified membrane association and precluded virus movement. We propose a topological model in which the TMV MP HRs intimately associate with the cellular membranes, allowing maximum exposure of the hydrophilic domains of the MP to the cytoplasmic cellular components.

IMPORTANCE

To facilitate plant viral infection and spread, viruses encode one or more movement proteins (MPs) that interact with ER membranes. The present work investigated the membrane association of the 30K MP of *Tobacco mosaic virus* (TMV), and the results challenge the previous topological model, which predicted that the TMV MP behaves as an integral membrane protein. The current data provide greatly needed clarification of the topological model and provide substantial evidence that TMV MP is membrane associated only at the cytoplasmic face of the membrane and that neither of its domains is integrated into the membrane or translocated into the lumen. Understanding the topology of MPs in the ER is vital for understanding the role of the ER in plant virus transport and for predicting interactions with host factors that mediate resistance to plant viruses.

Positive-strand RNA plant viruses are dependent on the endoplasmic reticulum (ER) for translation, replication, and intercellular movement (1). Plant viruses encode one or more movement proteins (MPs) that enable viral propagation from the initial infected cells to the uninfected neighboring cells. For cell-to-cell transport, viruses exploit the plasmodesmata (PD), which contain ER membrane prolongations that connect plant cells. Numerous studies have expanded our insight into the cellular mechanisms permitting the intracellular and intercellular transport of plant viruses, with *Tobacco mosaic virus* (TMV) being strongly represented in the pioneering research and in a large proportion of the reported data. The proteins implicated in the TMV genome replication are produced from the viral genomic RNA (vRNA), while the movement and capsid proteins are produced from two different subgenomic RNAs. TMV MP is necessary for local spread of TMV through the PD. Studies have identified which residues/domains participate in each of the multiple functions assigned to TMV MP, e.g., RNA binding (2), localization on PD (3, 4), increasing the PD size exclusion limit to facilitate viral genome translocation (5–7), and associating with ER membranes at replication sites during earlier infection stages and with microtubules and microfilaments of the cytoskeleton for transporting the ER-associated viral replication complex to PD (8–10).

TMV MP is the type member of the 30K family, a group of MPs from viruses belonging to 18 different genera that each express a unique MP with a molecular mass of approximately 30 kDa. TMV MP associates with the ER membrane in the early stage of infection, inducing structural changes (11). Viral replication starts within proximity of the ER membrane; shortly after translation of the first viral proteins, the virus rearranges the intracellular membranes to form the so-called "viral factories," a process to which the MP is fundamental (12, 13). The viral factories are ER-derived membranous compartments that house concurrent virus replication and synthesis and accumulation of viral proteins (14). The MP also participates in localizing the vRNA into the ER extensions that reach and cross the PD and can temporarily control PD gating to facilitate vRNA passage into a noninfected adjacent cell (7). Therefore, the association of the movement protein with the ER membrane is fundamental for the cell-to-cell movement of the vRNA.

Previous studies have demonstrated that TMV MP is not released from cellular membranes after urea (2.5 M) or NaCl treatment (11). Additionally, TMV MP holds a trypsin-resistant core, containing two hydrophobic regions (HRs) (15). Based on results

Received 9 December 2013 **Accepted** 20 December 2013
Published ahead of print 26 December 2013
Editor: A. Simon
Address correspondence to Ismael Mingarro, Ismael.Mingarro@uv.es, or Jesús A. Sánchez-Navarro, jesanche@ibmcp.upv.es.
A.P. and L.M.-G. contributed equally to this work.

doi:10.1128/JVI.03648-13

of circular dichroism spectroscopy of urea- and SDS-solubilized TMV MP and trypsin digestion followed by mass spectroscopy, a topological model was proposed in which TMV MP behaves as an integral ER membrane protein, with the N and C termini exposed to the cytoplasm and two transmembrane (TM) regions connected by a hydrophilic loop translocated into the ER lumen (15, 16). However, this topological working model cannot explain several TMV MP properties. Some RNA-binding domains (2) or interactions with microtubules (9, 17), chaperones (18), or cell wall-associated proteins (19) rely on TMV MP regions that are not accessible in the current model. Further investigations of the interaction of MPs with cellular membranes are needed to obtain a more complete understanding of the role of MPs in virus infection and cell-to-cell spread.

In the present study, we used biochemical and cellular approaches to demonstrate that TMV MP hydrophobic regions (HRs) do not span biological membranes, either when isolated or in the full-length protein context. Taking these results together with the behavior of the protein in response to different chemical treatments, the results of bimolecular fluorescence complementation (BiFC) studies, and the results of viral cell-to-cell movement assays, we propose that the TMV MP peripherally associates with ER membranes in living plant cells.

MATERIALS AND METHODS

Computer-assisted analysis of TM helices. TM helices for the TMV MP sequence were predicted using some of the most commonly used prediction methods available on the Internet. All user-adjustable parameters were left at their default values.

DNA manipulations. The TMV MP wild-type (wt) (plasmid provided by S. Chapman, Scottish Crop Research Institute [SCRI]) (20) and Lep (21) genes were amplified using PCR with specific sense and antisense primers containing the appropriate restriction enzyme sequences. The plasmid pGEM-TMVMP was created by subcloning the amplified TMV MP fragment into the pGEM-Lep vector using the NcoI/NdeI restriction sites. The HRs from TMV MP were introduced between SpeI and KpnI sites in a previously modified Lep sequence from the pGEM1 plasmid (Promega) (22, 23). The QuikChange mutagenesis kit from Agilent Technologies (La Jolla, CA) was used to engineer the glycosylation sites G3 (Lep residues 277 to 279) and G3′ (Lep residues 108 to 110) and to insert four leucine or four aspartate residues into the different plasmids (see below).

To fuse the hemagglutinin (HA) sequence at the C termini of both proteins, the amplified TMV MP or Lep fragments were subcloned in the pSK+35S-MPPNRSV:HA construct (21) replacing the *Prunus* necrotic ringspot virus (PNRSV) MP gene. The resultant clones, pSK+35S-TMVMP:HA and pSK+35S-Lep:HAt, contained the corresponding protein fused to the HA epitope under the control of 35S promoter from cauliflower mosaic virus (CaMV) and the inhibitor II terminator from the potato proteinase. Then, the expression cassettes 35S-TMVMP:HA and 35S-Lep:HA were subcloned into the pMOG800 binary vector by using the restriction enzyme XhoI. To fuse the N-terminal 154 amino acids of the yellow fluorescent protein (NYFP) to the N or C terminus of the TMV MP or Lep proteins, we first introduced the full-length MP or Lep genes into pSK+35S-EGFP (24) by replacing the enhanced green fluorescent protein (EGFP) gene. The resultant clones (pSK+35S-TMVMP and pSK+35S-Lep) were used to introduce the NYFP at the N or C terminus of the protein. To do this, the NYFP sequence was subcloned into NcoI or NheI restriction sites of the pSK+35S-TMVMP vector, resulting in the pSK+35S-NYTMVMP and pSK+35S-TMVMPNY constructs (see Fig. 3A). Additionally, the clone pSK+35S-TMVMP was modified, using site-directed mutagenesis, to create an EcoRI restriction site, which allows the insertion of the NYFP after residue 104 of TMV MP. The resultant pSK+35S-TMV<NY>MP clone would have the NYFP between the HRs. Finally, the expression cassettes 35S-NYTMVMP, 35S-TMVMPNY, and 35S-TMV<NY>MP were subcloned inside the pMOG800 binary vector by using the restriction enzyme SacI. The clone pSK+35S-NYTMVMP was used as a template to amplify the NYFP fused to the C terminus of the N-terminal 104-amino-acid sequence of the TMV MP with specific primers generating pSK+35S-TMVHR1NY. The amplified fragment was used to replace the EGFP gene in the plasmid pSK+35S-EGFP, using the NcoI and Eco47III restriction sites, resulting in the clone pSK+35S-NYTMVHR1. Its expression cassette was introduced into the pMOG800 binary vector by using the SacI site.

The clone pSK+35S-TMVHR1NY was used as a template for site-directed mutagenesis to insert four leucine or aspartic acid residues after residue 69 of the TMV MP (see Fig. 5). The corresponding expression cassettes (35S-TMVHR1L4NY and 35S-TMVHR1D4NY) were inserted into pMOG800, as described above.

In order to insert the NYFP fragment between the TM domains (H1 and H2) from Lep, codon 122 of the Lep DNA sequence (included in the clone pSK+35S-Lep) was modified, using site-directed mutagenesis, to create a BglI restriction site. At the same time, the NYFP fragment was amplified using specific primers, and it was introduced into the plasmid pSK+35S-Lep, which had previously been digested with BglI and dephosphorylated, resulting the clone pSK+35S-Lep<NY>P1 (see Fig. 4). Finally, the expression cassette was subcloned, using SacI, in the pMOG800 binary vector. The clone pSK+35S-Lep<NY>P1 was used as a template to amplify the NYFP fragment fused to the C terminus of the 61 N-terminal amino acids from Lep. The PCR product amplified had the EGFP gene of the pSK+35S-EGFP construct inserted by using the NcoI and Eco47III restriction sites, resulting in the clone pSK+35S-TM1LepH1NY. Finally, this expression cassette was subcloned, upon digestion with SacI, in the pMOG800 binary vector. PNRSV constructs were produced similarly starting from the previously described 35S-PNRSVMP:HA-PoPit cassette (21).

The expression cassettes, which contained the N- and C-terminal fragments targeting the endoplasmic reticulum lumen ($NYFP_{ER}$ and $CYFP_{ER}$) corresponded to the clones pRT-YN-ER and pRT-YC-ER (provided by Jari P. T. Valkonen, Department of Applied Biology, University of Helsinki, Helsinki, Finland) (25). These cassettes were subcloned into the vector pMOG800. Binary vectors expressing N and C termini of the YFP targeting the cytosol ($NYFP_{cyt}$ and $CYFP_{cyt}$) were provided by F. Aparicio (Instituto Biología Molecular y Celular de Plantas Primo Yúfera, Valencia, Spain) (26). All DNA manipulations were confirmed by plasmid DNA sequencing.

To introduce four leucine or four aspartate codons in the TMV MP gene of an infectious TMV-based vector expressing the DsRed protein, the pDsRedTMV-wt plasmid (provided by S. Chapman, Scottish Crop Research Institute) (20) was modified by site-directed mutagenesis as described above to create the pDsRedTMV-HR1L4 and pDsRedTMV-HR1D4 constructs, respectively.

***In vitro* protein expression.** Lep-derived constructs and the full-length TMV MP were transcribed and translated in the presence of reticulocyte lysate, [^{35}S]Met, and dog pancreas rough microsomes (RMs) as described previously (21). Samples were analyzed by sodium dodecyl sulfate-polyacrylamide gel electrophoresis (SDS-PAGE), and the gels were visualized on a Fuji FLA3000 phosphorimager using ImageGauge software. The extent of glycosylation of a given mutant was calculated as the quotient of the glycosylated band intensity divided by the summed intensities of the glycosylated and nonglycosylated bands for each lane analyzed.

The proteinase K digestions were performed after *in vitro* translation by incubation the mixture with 400 μg/ml proteinase K on ice for 40 min. The reaction was stopped by adding 2 mM phenylmethylsulfonyl fluoride. The membrane fraction was then collected by centrifugation and analyzed by SDS-PAGE.

Membrane sedimentation, alkaline wash, and urea treatment. The translation mixture was diluted in 8 volumes of buffer A (35 mM Tris-HCl at pH 7.4 and 140 mM NaCl) for membrane sedimentation or 4 volumes of buffer A supplemented with 100 mM Na_2CO_3 (pH 11.5) for the alkaline wash. The samples were incubated on ice 30 min and clarified by centrifugation (10,000 × *g*, 20 min). Membranes were collected by ultracentrifugation (100,000 × *g*, 20 min, 4°C) of the supernatant onto a 50-μl sucrose cushion. Pellets (P) and supernatants (S) of the ultracentrifugation were analyzed by SDS-PAGE.

Membrane flotation. We examined the membrane association of the full-length TMV MP using vesicle flotation (21). The translation mixture was adjusted with 0.2 M Na_2CO_3 (pH 11.5) to a final volume of 250 μl and incubated for 1 h on ice. Samples were then mixed with 4 M sucrose–0.1 M Na_2CO_3 to obtain a 1.8 M sucrose solution. The sucrose mixture was transferred to centrifugation tubes and overlaid with 275 μl of 1.25 M sucrose–0.1 M Na_2CO_3 and with 250 μl of 0.25 M sucrose–0.1 M Na_2CO_3. After centrifugation for 4 h in a Beckman TLS-55 rotor, four fractions of approximately 200 μl were withdrawn from the top and analyzed by SDS-PAGE. The pellet was dissolved with the last 200-μl fraction. Results were always processed in parallel with the sample distribution of the model membrane protein Lep (the leader peptidase from *E. coli*).

Expression of TMV MP and Lep proteins *in planta*, membrane sedimentations, and Western blot assay. *Agrobacterium tumefaciens* (strain C58) cultures were transformed with both binary pMOG800 plasmids, containing the 35S-TMVMP:HA and 35S-Lep:HA expression cassettes. The cultures at an optical density at 600 nm (OD_{600}) of 0.4 were infiltrated into *Nicotiana benthamiana* plants as previously described (24). At 3 days postinfiltration, the leaves were processed to obtain enriched membrane fractions as described previously (27). The resultant membrane-enriched pellet was resuspended in buffer A (20 mM HEPES [pH 6.8], 150 mM potassium acetate, 250 mM mannitol, 1 mM $MgCl_2$, 2.5 μl of protease inhibitor cocktail for plant cell and tissue extracts; Sigma) and divided into three aliquots to be left untreated or to be subjected to the alkaline wash and urea treatments as described previously. Membranes were collected by ultracentrifugation (100,000 × *g*, 20 min, 4°C). All the fractions were analyzed by Western blotting in 12% SDE-PAGE gels. The gel was electrotransferred to polyvinylidene difluoride membranes following the manufacturer's instructions (Amersham). The proteins tagged with the HA epitope were detected by using an anti-HA (Sigma) antibody and a secondary antibody conjugated with peroxidase (Sigma). The chemibioluminescence detection was made using the substrate recommended by Amersham (ECL Plus Western blotting detection system).

Bimolecular fluorescence complementation assays. In bimolecular fluorescence complementation (BiFC) assays, the different proteins (see Fig. 3 to 5) were transiently expressed with the C-terminal YFP fragment targeting the cytosol (CYFPcyt) or the lumen of the ER (CYFPER). For this, *Agrobacterium tumefaciens* (strain C58) cultures (OD_{600} = 0.4) transformed with the corresponding binary pMOG800 plasmids were used to infiltrate *N. benthamiana* plants as previously described (24). The plants were kept at 24°C during the day and 18°C at night, with a 16-h/8-h day/night photoperiod. At 4 days postinfiltration, the fluorescence reconstitution was monitored in a confocal Leica TCS SL microscope (λ [excitation] = 488 nm; λ [emission] = 500 to 550 nm).

Inoculation of *Nicotiana benthamiana* plants. pDsRedTMV-wt and the corresponding derivatives, containing four leucine (pDsRedTMV-HR1L4) or four aspartate (pDsRedTMV-HR1D4) residues after residue 69 of the MP gene, were linearized with KpnI and transcribed with T7 RNA polymerase. The infectious TMV transcripts were inoculated onto *N. benthamiana* leaves, and the fluorescent signal was monitored at 4 days postinoculation with a confocal Leica TCS SL microscope (λ [excitation] = 556 nm; λ [emission] = 570 to 650 nm).

RESULTS

Isolated TMV MP hydrophobic regions are not inserted into biological membranes. The TMV MP amino acid sequence was parsed to test the performance of several commonly used algorithms for predicting membrane-spanning regions. The predicted outcome (Table 1) varied greatly according to the method used, likely due to the limited hydrophobicity of the two HRs of TMV MP. To test these predictions, we assayed the membrane insertion capabilities of these HRs (Fig. 1A) using an *in vitro* experimental system based on the *Escherichia coli* inner membrane protein leader peptidase (Lep) (22), which accurately determines the integration of TM helices into ER membranes. Lep consists of two TM segments (H1 and H2) connected by a cytoplasmic loop (P1) and a large C-terminal domain (P2). It is inserted into ER-derived rough microsomal membranes (RMs) with both termini located in the lumen (Fig. 1B, left). The analyzed segment (HR tested) is engineered into the luminal P2 domain and is flanked by two acceptor sites (G1 and G2) for *N*-linked glycosylation (Fig. 1B, center and right). Single glycosylation (i.e., membrane integration) results in a molecular mass increase of ~2.5 kDa relative to the observed molecular mass of Lep expressed in the absence of microsomes. A molecular mass shift of ~5 kDa occurs upon double glycosylation (i.e., membrane translocation of the HR-tested). This system has the obvious advantage that the insertion assays are performed in the context of a biological membrane.

TABLE 1 Computer analysis of the TMV MP amino acid sequence

Algorithm	No. of TM segments	Position in[a]: HR1	HR2
DAS	2	65–75	155–165
Δ*G* prediction	2	61–80	148–167
HMMTOP	1		148–166
MEMSAT3	1		153–168
OCTOPUS	0		
SOSUI	0		
TMHMM	0		
TMpred	2	58–76	150–166
TopPred	2 (1 certain)	61–81[b]	146–166

[a] Starting amino acid–ending amino acid.
[b] Putative.

We found that translation of the chimeric constructs harboring the predicted TMV MP hydrophobic regions resulted in double-glycosylated forms (Fig. 1C, lanes 4 and 5), consistent with the translocation of these regions into the ER lumen, as expected according to the predicted apparent free energy (ΔG_{app}) of insertion (Fig. 1A). Figure 1C (lanes 1 to 3) shows control constructs with computer-designed previously tested translocation and integration sequences (28, 29), which produced the expected double- and single-glycosylation patterns, respectively.

Previous studies have shown that, in some cases, a neighboring TM helix can promote membrane insertion of a poorly hydrophobic TM region (30–33). Therefore, we used the *in vitro* system to investigate the insertion of the two HRs connected by their native loop (residues 61 to 167, shown in gray) (Fig. 1D). In these constructs, translocation of the full MP region across the microsomal membrane should result in modification of both G1 and G2 sites (Fig. 1D, center). However, insertion of both HRs into the membrane should result in only G1 receiving a glycan, because, as previously demonstrated (33), G2 in these constructs was too close to the membrane to be efficiently glycosylated (Fig. 1D, left). If only one of the two HRs was inserted, only G1 was modified; however, in that case, the large P2 domain was not translocated across the

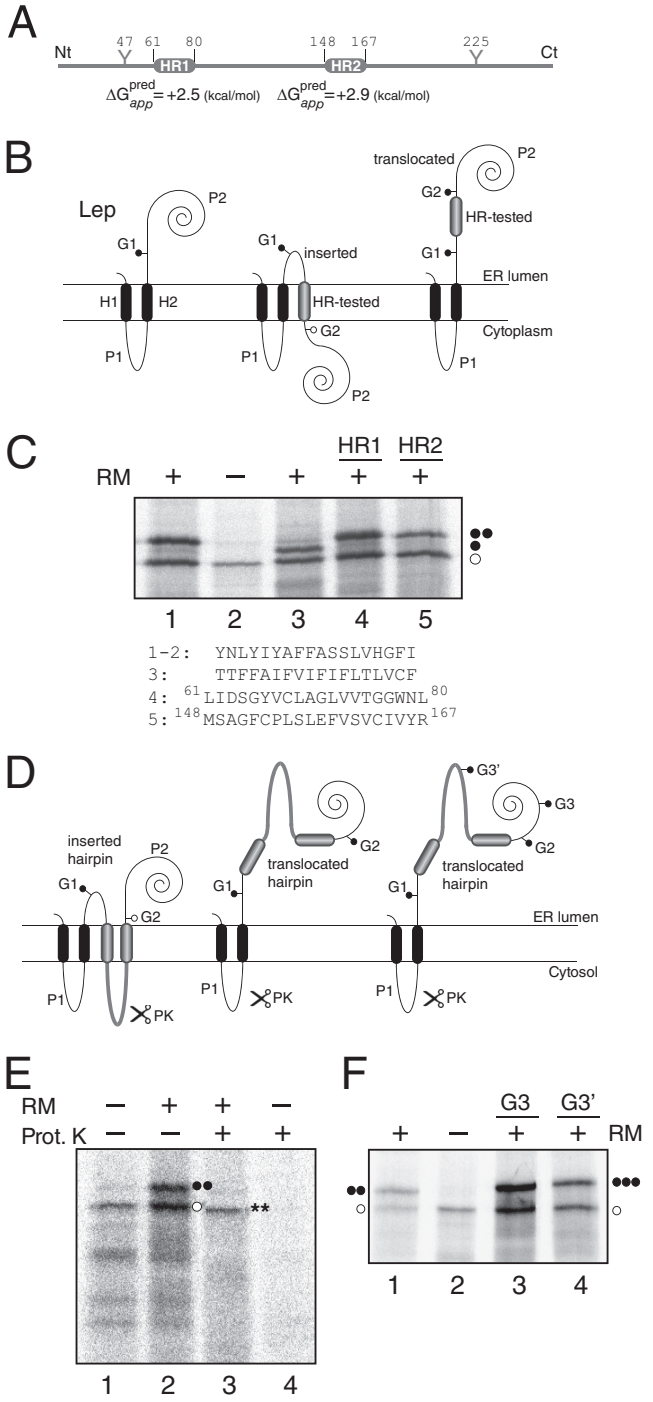

FIG 1 TMV-isolated HRs do not span ER-derived membranes. (A) Schematic representation of the TMV MP, highlighting the HRs (gray boxes). Y-shaped symbols denote potential (nonnaturally modified) glycosylation sites. Predicted ΔG_{app} values were estimated using the ΔG prediction algorithm available on the Internet (http://dgpred.cbr.su.se/). In this algorithm, positive values indicate translocation across the membrane (i.e., absence of stable insertion). (B) Schematic representation of the model leader peptidase (Lep) construct (left) and the variants used to report TMV MP HR1 and HR2 insertion into (center) or translocation across (right) the ER membrane. (C) *In vitro* translation of the different Lep constructs. Lep constructs containing TMV MP HR1 or HR2 were transcribed and translated in the presence of rough microsomal (RM) membranes (lanes 4 and 5, respectively). Control HRs were used to verify sequence translocation (in the presence or in the absence of RMs; lanes 1 and 2, respectively) and membrane integration (lane 3). The HR sequence in each construct is shown at the bottom. Nonglycosylated protein bands are indicated by a white dot, while singly and doubly glycosylated proteins are indicated by one and two black dots, respectively. (D) Schematic representations of topographical models for the in-block insertion (left) or translocation (center and right) of the two TMV MP HRs (residues 61 to 167) into the Lep sequence. Recognition by the translocation machinery of the two HRs as an integrating domain locates G1 and G2 at the luminal side of the ER membrane, but the short distance to the membrane prevents G2 glycosylation (left). The Lep chimera will be doubly glycosylated when this domain is translocated into the lumen of the microsomes (center). An additional glycosylation site was engineered either at the C-terminal P2 domain (G3) or at the hydrophilic loop (G3′) connecting HR1 to HR2 (right). (E) *In vitro* translation in the presence (+) or absence (−) of RMs and PK of Lep derivatives. The protected doubly glycosylated fragment is indicated by two asterisks. (F) *In vitro* translation of Lep-derived constructs harboring a third glycosylation site either at the C-terminal P2 domain (G3) (lane 3) or at the loop connecting HR1 and HR2 (G3′) (lane 4). Control hairpin samples are included (lanes 1 and 2). Triple-glycosylated forms are indicated by three black dots. All the gels are representative of at least 3 independent experiments.

microsomal membranes. In Fig. 1E, lanes 1 and 2 show that *in vitro* synthesis of this construct exclusively yielded double-glycosylated forms of the protein, suggesting the translocation of the TMV domain.

Proteinase K (PK) treatment of translation mixtures in the presence of microsomes should degrade the membrane protein domains that protruded into the cytosol but should not digest membrane-embedded or luminally exposed domains. PK treatment of these split translation reaction mixtures yielded protected forms that contained H2 and P2 domains from Lep, plus the fused MP region derived from the double-glycosylated molecules (Fig. 1E, lane 3). We also engineered an additional glycosylation site at the C-terminal P2 domain (G3) (Fig. 1D, right) or at the loop connecting the two HRs from the TMV MP sequence (G3′). As seen in Fig. 1F, both protein constructs were triple glycosylated, indicating that the full TMV MP region was translocated. Overall, these data suggest that, in the context of the Lep-derived model protein, the two HRs of TMV MP are not inserted into biological membranes.

TMV MP peripherally associates with membranes *in vitro* and *in vivo*. Next, we analyzed the insertion of full-length TMV MP into the membrane. The protein sequence includes two potential glycosylation sites at the N- and C-terminal domains (positions 47 and 225) (Fig. 1A), which can be used as topological reporters in translation assays. We found that translation in the presence of RMs yielded nonglycosylated molecules that were totally sensitive to PK treatment (Fig. 2A, lanes 4 to 6), regardless of the presence of microsomal membranes. Furthermore, *in vitro* translation of a version of TMV MP carrying an engineered glycosylation site (at residue 108) in the hydrophobic loop connecting the HRs similarly yielded nonglycosylated molecules that were sensitive to PK treatment (data not shown). As a control, the translation of Lep, which carries a single glycosylation site at the P2 domain, in the presence of membranes yielded a mainly glycosylated population (Fig. 2A, lane 2) and a protected, glycosylated H2-P2 fragment upon PK treatment (Fig. 2A, lane 1). These results indicated that no domain of the TMV protein was translocated into the microsomal lumen or inserted into the microsomal membrane.

However, isolation of microsomal membranes after *in vitro* translation showed that TMV MP was mostly present in the membrane-rich fraction (86.4%) (Fig. 2B, lanes 1 and 2), suggesting a

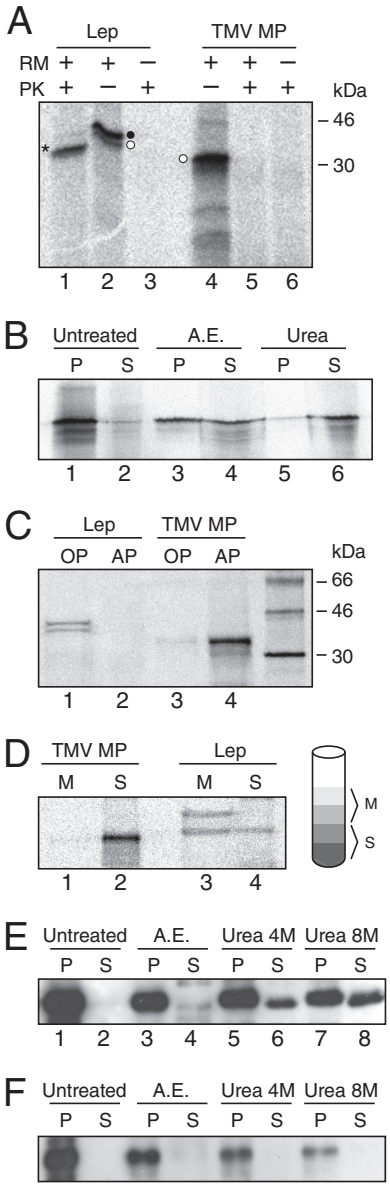

FIG 2 TMV MP association with biological membranes. (A) Proteinase K (PK) treatment of microsomes carrying *in vitro* translated wild-type Lep (lanes 1 to 3), and the full-length TMV MP (lanes 4 to 6). Nonglycosylated and glycosylated molecules are indicated by white and black dots, respectively. An asterisk indicates protease-protected fragments. (B) Segregation of [^{35}S]Met-labeled TMV MP into membrane and soluble fractions (untreated) and after alkaline extractions (A.E.; sodium carbonate buffer wash) or urea treatments (8 M). P and S denote pellet and supernatant, respectively. (C) Triton X-114 partitioning of Lep (lanes 1 and 2) and TMV MP (lanes 3 and 4). OP and AP refer to organic and aqueous phases, respectively. (D) Flotation gradient centrifugation of TMV MP (lanes 1 and 2) and Lep (lanes 3 and 4) translated *in vitro* in the presence of RMs. M and S denote membrane and soluble fractions, respectively. (E) Segregation into membrane and soluble fractions of *in planta*-expressed TMV MP. HA-tagged TMV MP was expressed in *N. benthamiana* plants by agroinfiltration. Comparable P and S fractions obtained from membrane fractions, untreated and after alkaline wash or urea treatments (4 M or 8 M), were analyzed by Western blot analysis using an anti-HA antibody. (F) HA-tagged Lep was expressed in *N. benthamiana* plants by agroinfiltration and analyzed as for panel E.

tight association with cellular membranes. To identify the type of interaction, we first washed the translation mixture with sodium carbonate (pH 11.5), a treatment that is known to transform microsomes into membranous sheets, releasing soluble luminal proteins (27). After the alkaline treatment, TMV MP remained mainly associated with the membrane-rich fraction (58.8%). Next we washed the membranes with 8 M urea, a treatment that should release all polypeptides from the membrane except the integral membrane proteins (21). With this treatment, the great majority of the protein was extracted in the supernatant fraction (87.8%) (Fig. 2B, lanes 5 and 6). These results suggest a tight but peripheral association of TMV MP with the microsomal membranes. The translation reaction mixtures were also treated with Triton X-114, a nonionic detergent that forms a separate organic phase, segregating the membrane lipids and hydrophobic proteins from the aqueous phase containing nonintegral membrane proteins (34). After phase partitioning, the TMV MP was detected in the aqueous but not the organic phase (Fig. 2C). As expected, Lep was recovered from the organic phase. These results supported the idea that TMV MP is not an integral membrane protein. We also used vesicle flotation assays to examine the membrane association of TMV MP. Translation of TMV MP in the presence of RMs followed by flotation gradient centrifugation showed that the protein was exclusively recovered from the bottom fractions of the gradient (S fractions) (Fig. 2D, lanes 1 and 2), confirming that the TMV MP was not an integral membrane protein. Parallel control experiments using Lep demonstrated the presence of Lep in the upper membrane-associated fractions of the gradient (M fractions) (Fig. 2D, lanes 3 and 4).

Finally, we studied the membrane association of TMV MP in the natural host *Nicotiana benthamiana*. The plants were infiltrated with *Agrobacterium tumefaciens* cultures carrying the pMOG35S-TMVMP:HA construct, which transiently expressed TMV MP fused to the HA epitope. Total proteins were extracted from *N. benthamiana* agroinfiltrated leaves at 3 days postinfiltration. A membrane-rich fraction was generated by centrifugation at 100,000 × *g* (Fig. 2E, lanes 1 and 2) and was subjected to the above-described chemical treatments. The results showed that the TMV MP remained associated with the membrane fraction after sodium carbonate treatment (94.6%) (Fig. 2E, lanes 3 and 4). However, more aggressive treatments (4 M and 8 M urea) led to the detection of some TMV MP in the soluble fraction (27.4% and 44.3%, respectively). Parallel experiments using HA-tagged Lep as an integral membrane protein control showed Lep accumulation exclusively in the membrane fractions following these treatments (Fig. 2F).

Together, these results suggest that TMV MP, rather than being an integral membrane protein, is a peripherally associated membrane protein, with the full-length molecule being oriented toward the cytoplasm both *in vitro* and *in planta*.

ER membrane association of TMV MP in living plant cells. We next analyzed TMV MP membrane disposition using bimolecular fluorescence complementation (BiFC) assays (35). This technique relies on the capacity of two nonfluorescent fragments, the N (NYFP; 1 to 154 amino acids) and C (CYFP; 155 to 239 amino acids) termini of the yellow fluorescent protein (YFP), to interact with each other when they are overexpressed in the same subcellular compartment (25). One YFP fragment was targeted to the cytosol ($NYFP_{cyt}$ or $CYFP_{cyt}$) or to the ER lumen ($NYFP_{ER}$ or $CYFP_{ER}$), and it was coinfiltrated with the counterpart YFP

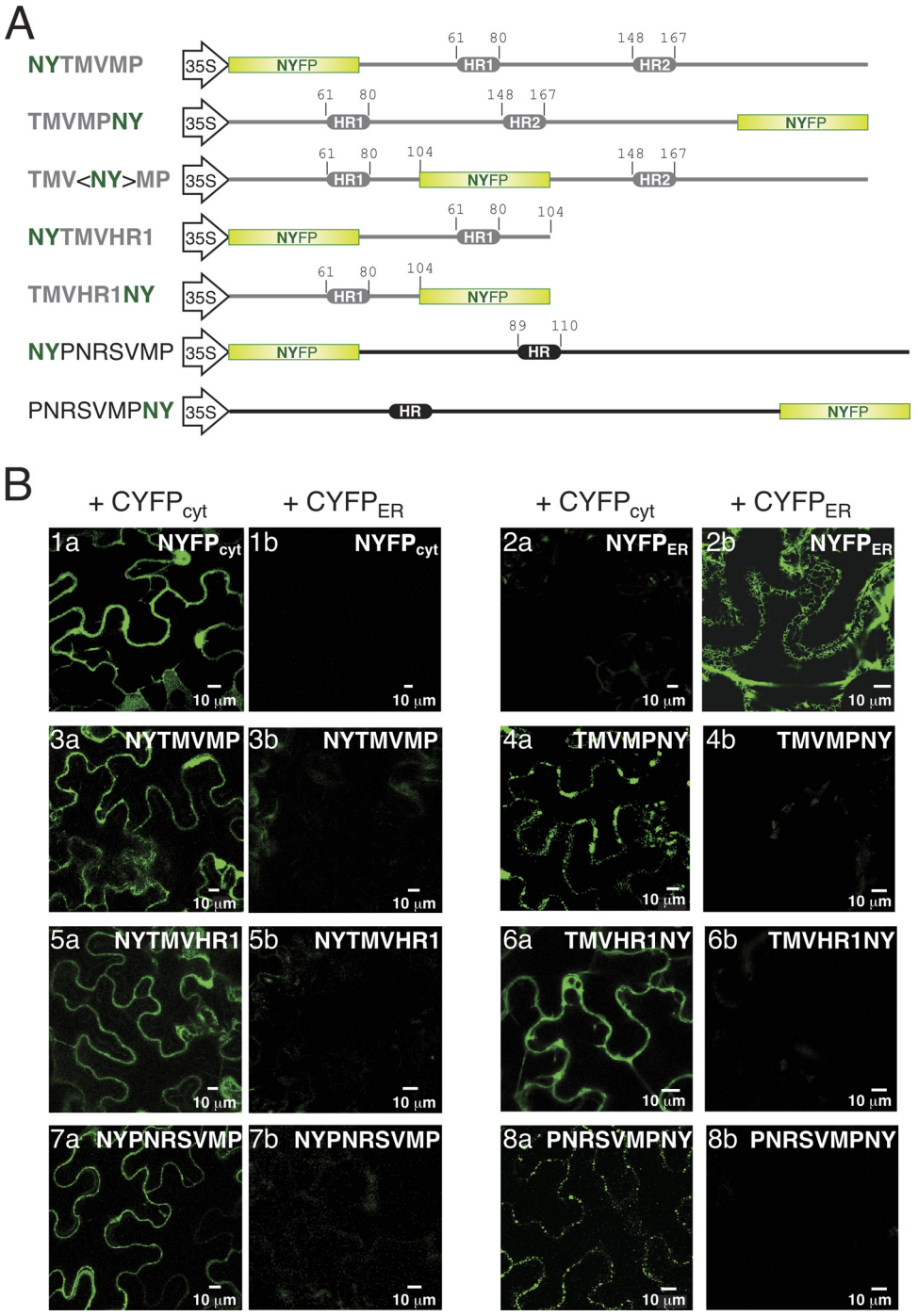

FIG 3 ER membrane association of TMV MP in living plant cells. (A) Schematic representation of expression cassettes used for BiFC. (B) Fluorescence observed *in planta* after transient expression of the constructs depicted in panel A plus the C-terminal YFP fragment targeting the cytosol (CYFP$_{cyt}$) (A) or the lumen of the ER (CYFP$_{ER}$) (B). Images reveal the topology of the N terminus (panels 3a, 3b, 5a, and 5b), the C terminus (4a and 4b), and the region located between the two HRs (6a and 6b) of the TMV MP. The topology of the N and C termini of the PNRSV MP is also shown in panels 7a and b and panels 8a and b, respectively. Positive and negative controls are shown in panels 1a and 2b and panels 1b and 2a, respectively. The fluorescence was monitored at 4 days postinfiltration using a confocal Leica TCS SL microscope.

fragment attached to the N or C terminus of the TMV MP or inserted into the central hydrophilic loop connecting the two HRs (Fig. 3A). Reconstitution of the fluorescence-competent YFP structure indicated the *in vivo* localization of the fused/inserted YFP fragment in the appropriate compartment. As expected, no fluorescence was detected in leaves that had been agroinfiltrated with NYFC or CYFC, whereas fluorescent cells were readily found in leaves coinfiltrated with the NYFP and CYFP constructs targeted to the same subcellular compartment (Fig. 3B, panels 1a, 1b, 2a, and 2b). Next, the NYFP (NY) was fused to the N terminus

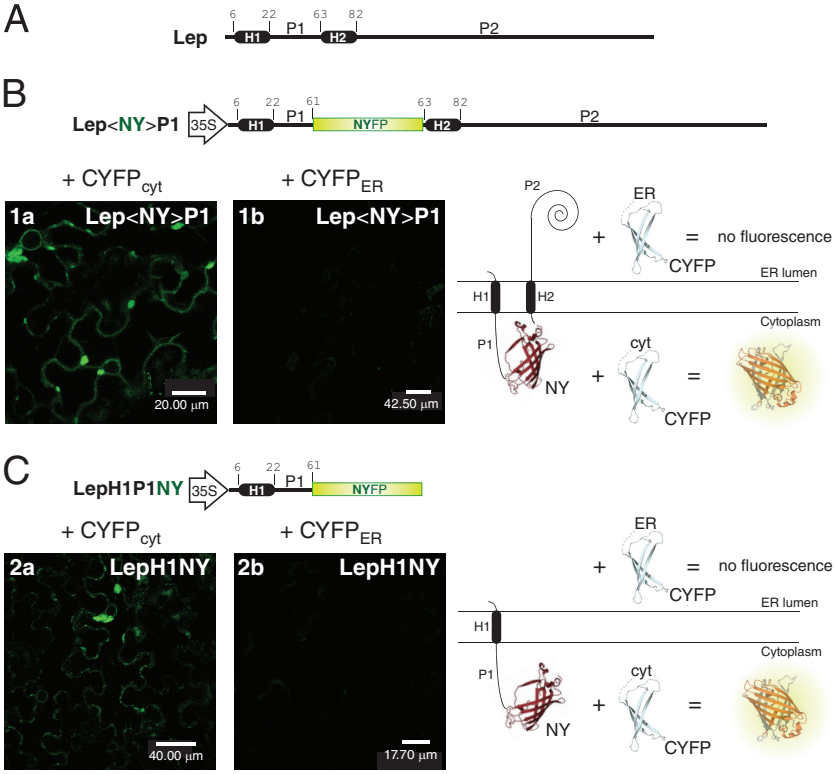

FIG 4 ER membrane association of Lep in living plant cells. (A) Schematic representation of the Lep protein. (B) (Top) Schematic representation of expression cassette used for BiFC. (Bottom left) Fluorescence observed *in planta* after transient expression of the indicated construct, in which the N terminus of YFP was inserted within the P1 domain after residue 61 in the Lep sequence, plus the C-terminal YFP fragment targeting the cytosol (CYFP$_{cyt}$) (panel 1a) or the lumen of the ER (CYFP$_{ER}$) (panel 1b). (Bottom right) Schematic of the BiFC assay. The expression of the YFP fragments in the same compartment facilitates their association, allowing the formation and maturation of the fluorophore, which consequently leads to emission of fluorescence. (C) (Top) Schematic representation of expression cassette used for BiFC, which included the 61 N-terminal residues of Lep. (Bottom left) Fluorescence observed *in planta* after transient expression of the construct represented on top. (Bottom right) Schematic of the BiFC assay. Images reveal the topology of the P1 domain from Lep both in the full-length construct (B) and in the truncated Lep molecules (C). The fluorescence was monitored at 4 days postinfiltration using a confocal Leica TCS SL microscope.

(NYTMVMP), to the C terminus (TMVMPNY), or between both HRs (TMV<NY>MP, after residue 104) of TMV MP (Fig. 3A). Every chimeric protein was coinfiltrated with the corresponding expression cassette for the CYFP$_{cyt}$ or CYFP$_{ER}$ fragment in *N. benthamiana* plant leaves. With the constructs NYTMVMP and TMVMPNY, fluorescence reconstitution was exclusively observed when both chimeric proteins were coexpressed with CYFP$_{cyt}$ (Fig. 3B, panels 3a and 4a), indicating that both N and C termini of the TMV MP were oriented toward the cytosol. With TMV<NY>MP, fluorescence was not observed in the ER or in the cytosol, suggesting that the fused NYFP was likely inaccessible for interaction with its partner, regardless of the partner (CYFP) location. Similar analysis with the Lep protein (Fig. 4A), in which the NYFP fragment was fused at the P1 domain, revealed a clear fluorescence signal in the expected cytosol compartment (Fig. 4B).

To unravel the subcellular location of the central hydrophilic loop of TMV MP, we fused the NYFP fragment to the N or C terminus of truncated MP versions (Fig. 3A), thus reducing the putative accessibility problem of the YFP fragment in the TMV<NY>MP construct. We fused the NYFP fragment to either the N or C terminus of the 104 N-terminal amino acid residues of the viral protein (Fig. 3, NYTMVHR1 and TMVHR1NY, respectively), which included HR1 plus 24 amino acid residues of the hydrophilic loop region that have been proposed to translocate into the ER lumen (15). Figure 3 shows that both NYTMVHR1 and TMVHR1NY chimeras reconstituted the fluorescence only with the CYFP$_{cyt}$ (Fig. 3B, panels 5a and 6a), indicating that the loop between HR1 and HR2 was oriented toward the cytosol. Additionally, the N terminus of the TMV MP truncated molecule maintained its cytosolic orientation, as observed for the full-length protein. Parallel experiments were conducted using a truncated version of Lep that included the first TM segment (H1) and the P1 domain, which are the regions responsible for proper targeting and orientation of the Lep protein in eukaryotic membranes (36). The BiFC analysis revealed that Lep-truncated molecules (LepH1P1NY) oriented their P1 domain toward the cytosol (Fig. 4C), since only the cytoplasm-targeted CYFP partner restored fluorescence, similar to with the full-length Lep protein (Fig. 4B).

To further validate the topology observed, we used the BiFC technology to characterize the topology of PNRSV MP, another component of the 30K family. PNRSV MP is a peripherally associated membrane protein with a single HR that cannot span the membrane (21). The NYFP fragment was fused to the N (NYPNRSVMP) or C (PNRSVMPNY) terminus of PNRSV MP. The transient coexpression of the two PNRSV MP chimeric pro-

teins with the differently targeted CYFP fragments resulted in fluorescence reconstitution only with $CYFP_{cyt}$ (Fig. 3B, panels 7a and 8a), indicating that both the N and C termini of the PNRSV MP were located at the cytosol. These results agreed with the previous membrane association model proposed for PNRSV MP (21) and further supported the topology observed for the TMV MP. Altogether, these results indicated that no region of the viral TMV MP was translocated into the ER lumen, corroborating that neither the idea HR1 nor HR2 can span the membrane in living plant cells.

The membrane disposition of TMV MP can be modulated by altering HR1 hydrophobicity. Topological studies related to signal sequences or N-terminal TM segments have emphasized the relevance of the hydrophobicity of these domains in the overall orientation of the protein relative to the membrane (37, 38). The hydrophobicity of TMV MP HR1 was predicted to be low (+2.5 kcal/mol) (Fig. 1A), correlating with the experimental results obtained both *in vitro* and *in vivo* and explaining the observed peripheral association. To investigate whether altering HR1 hydrophobicity would modulate the membrane disposition of TMV MP, we designed two mutants with four leucine (HR1L4) or four aspartate (HR1D4) residues inserted roughly in the middle of the HR1 region (after residue 69). Figure 5A shows the insertion frequencies on the biological hydrophobicity scale (22, 39), which were predicted for these mutants using the ΔG prediction server v1.0 (http://dgpred.cbr.su.se/). In this algorithm, the predicted insertion frequency comes from the apparent free-energy difference (ΔG_{app}) from insertion into ER membranes. We first inserted these mutations in the Lep system (Fig. 1B) and tested their ability to be inserted into microsomal membranes. Translation of the HR1L4 construct in the presence of membranes produced doubly (~34%) and singly (~66%) glycosylated molecules (Fig. 5B, lane 2), indicating partial insertion of the HR1L4 domain, in agreement with its predicted value. As expected, the HR1D4 mutant retained its tendency to translocate, yielding only double-glycosylated molecules when translated in the presence of ER-derived membranes (Fig. 5B, lane 5). These results were further examined by PK treatment of the constructs, where a protease-protected fragment of the HR1D4 construct indicated membrane translocation (Fig. 5B, lane 6).

Subsequently, to analyze the effects of these mutations in living plant cells using BiFC assays, we inserted four leucine or aspartate residues in the TMVHR1NY construct. *A. tumefaciens* cultures coexpressing HR1L4NY or HR1D4NY with $CYFP_{cyt}$ or $CYFP_{ER}$ were coinfiltrated into *N. benthamiana* plants, as described above. At 2 days postinfiltration, the fluorescence reconstitution was monitored. Figure 5C shows that HR1D4NY oriented the split-NYFP molecule exclusively toward the cytosol (panels 2a and b). In contrast, fluorescence signals were detected in the samples prepared from leaves coexpressing the HR1L4NY construct and $CYFP_{cyt}$ (Fig. 5C, panel 1a) or $CYFP_{ER}$ (panel 1b). These data indicate that the presence of the leucine stretch partially promoted TM disposition of the HR1, translocating the C terminus into the ER, which nicely correlated with the insertion data obtained with the Lep system (Fig. 5B).

Finally, to study the potential effect of these mutations on cell-to-cell movement *in vivo*, a chimeric TMV construct carrying the DsRed fluorescent protein (20) (DsRedTMV-wt) was modified to introduce four leucine (DsRedTMV-HR1L4) or four aspartate (DsRedTMV-HR1D4) codons into the MP gene. The resultant transcripts were inoculated onto *N. benthamiana* leaves, and the fluorescence signal was monitored at 4 days postinoculation. The results revealed single fluorescent cells for the TMV constructs carrying the mutated MP gene, indicating that both modified MPs were incompetent to support the cell-to-cell transport of TMV (Fig. 5D).

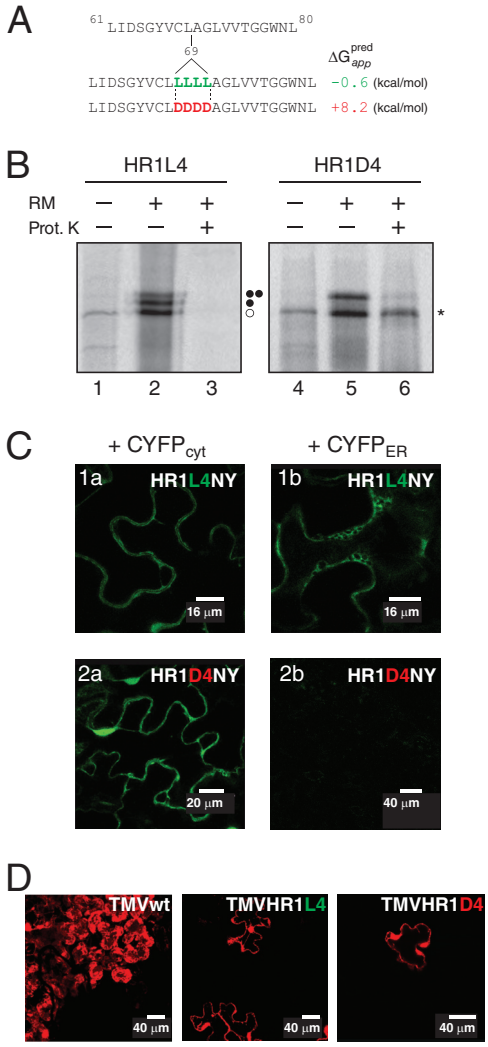

FIG 5 Effect of hydrophobicity on HR1 insertion into biological membranes. (A) HR1-derived sequences and the free energy that they require to adopt a TM conformation as calculated using the ΔG prediction algorithm (22, 39). (B) *In vitro* translation of the Lep-derived constructs (Fig. 1) in the presence of microsomal membranes and proteinase K, as indicated. Nonglycosylated protein bands are indicated by a white dot, and singly and doubly glycosylated proteins are indicated by one and two black dots, respectively. The protected doubly glycosylated fragment is indicated by an asterisk. The gels are representative of at least 3 independent experiments. (C) BiFC analysis of the *in planta* topology of the C terminus of the N-terminal 104 aa of the TMV MP carrying four leucine (HR1L4NY) or four aspartate (HR1D4NY) residues in the HR1 region. The expression cassette TMVHR1NY (depicted in Fig. 3A) was modified as indicated in panel A. The resulting constructs were transiently expressed *in planta* together with the C-terminal YFP fragment addressed to the cytosol ($CYFP_{cyt}$) (A) or the ER lumen ($CYFP_{ER}$) (B). (D) Detection of red fluorescence in *Nicotiana benthamiana* plants inoculated with infectious TMV transcripts carrying the MP wild type (DsRedTMV-wt) or its MP variants with four leucine (DsRedTMV-HR1L4) or four aspartate (DsRedTMV-HR1D4) residues introduced after amino acid 69. The fluorescence was monitored at 3 to 4 days postinfiltration/postinoculation using a confocal Leica TCS SL microscope.

DISCUSSION

Cellular membranes are a critical component of the virus cycle, for both replication and intra- and intercellular transport (1). During the virus life cycle, plant viral proteins associate with multiple membrane components, including the ER, Golgi, vacuolar, peroxisomal, chloroplast, mitochondrial, and endosomal vesicle membranes (40, 41). During virus transport, the virus uses the ER or the Golgi apparatus to reach the PD, which provides continuity between adjacent cells, allowing cell-to-cell vRNA movement. Movement proteins are key components connecting vRNA to cellular membranes. Understanding the topology of MPs in the ER is vital to understanding the role of the ER in PD transport and to predicting interactions with host factors that mediate resistance to plant viruses.

The MP of TMV has been proposed to be an ER-integral membrane protein with two TM regions (15). However, this suggestion was not supported by conclusive data (42). In the present work, we further characterized the TMV MP topology, with special emphasis on the two putative TM domains (15). Our *in silico* analysis (Table 1) confirmed the presence of two hydrophobic regions (HR1 and HR2) that practically corresponded to the two proposed TM domains; however, the positive values of ΔG_{app} predicted that they were not membrane integrated. In accordance with these predictions, the two HRs of TMV MP did not span biological membranes *in vitro* when assayed using a robust membrane protein insertion assay, either independently or as a unit, including both regions in the same chimeric Lep construct (Fig. 1). Similar results were observed with *in vivo* approaches using the BiFC technique. Unlike the results obtained with TMV MP, this *in vitro* Lep assay indicated that HRs predicted from other plant virus MPs span biological membranes (29, 43, 44). Interestingly, these membrane-spanning sequences belong to MPs from viruses in which cell-to-cell transport relies on the concerted action of two small MPs, no larger than 12 kDa, and membrane insertion of one of these two MPs is essential for virus movement (45). We also observed that the HRs of TMV MP did not span the membrane when the full-length TMV MP was used in the glycosylation and proteinase K digestion experiments.

These *in vitro* results indicated that the TMV MP is not an integral membrane protein but did not eliminate the possibility that the protein is intimately associated with membranes. Different biochemical treatments designed to distinguish between associated and integral membrane proteins revealed that the full-length TMV MP (expressed *in vitro* or *in vivo*) behaves as an associated membrane protein. Additionally, the BiFC analysis performed to determine the TMV MP topology, confirmed that the N- and C-terminal regions, and the region located between the two HRs were oriented toward the cytosol. When we substantially increased its hydrophobicity by insertion of four leucine residues, the first HR was partially integrated into the membrane. Altogether, these results support a model in which the TMV MP is peripherally associated with the ER membrane and oriented to the cytosol.

It is remarkable that most MPs belonging to the 30K family show a single hydrophobic domain by which the viral protein associates with membranes. Only MPs of TMV and other species belonging to the genus *Tobamovirus* show two HRs. The presence of a second HR in the protein likely results in a stronger association with the ER membranes, which is consistent with the requirement for a more aggressive treatment (8 M urea) to release the protein from the ER membranes than is needed for the PNRSV MP association (21). In this sense, the inaccessibility of $CYFP_{cyt}$ to the NYFP inserted between both HRs using the BiFC technique is in agreement with the inaccessibility of monoclonal antibodies addressed to HR1 region (79 to 89 residues) and the adjacent sequence (98 to 120 residues) (46), as both could be explained by the tight association of this region to the membrane. Similarly, membrane fractionation experiments on a series of TMV MP deletion mutants suggested that the protein is tightly associated with membranes from infected protoplasts through the two HRs (16). However, we cannot rule out the possibility that the tertiary structure of TMV MP could impede the availability of some regions.

The membrane topology proposed here for TMV MP should be compatible with previously described host factor interactions. Indeed, unlike the previous model, this model explains the interactions with α-tubulin (144 to 169 amino acids [aa]) (10), microtubules (47, 48), vRNA (112 to 185 aa) (2, 49), and pectin methylesterase (130 to 185 aa) (19), as well as the interaction between the closely related MP of the *Tomato mosaic virus* (ToMV) and the Tm-2 resistance gene product (50). Only the reported interaction with calreticulin, a protein located in the ER lumen (19), seems to be incompatible with a TMV MP located at the cytosolic surface of the ER membrane. However, while calreticulin was first identified as having a luminal subcellular location at the ER (51), plant calreticulins have also been found outside the ER compartment, including on the Golgi apparatus and cell surface (52) or cytosol and nucleus (53), permitting the hypothesis that the TMV MP-calreticulin interaction is compatible with the MP topology proposed herein.

Overall, the obtained results obtained here suggest a new topological model for the TMV MP, in which the MP is associated with the cytosolic surface of the ER membranes. This model is in agreement with the topology reported for other members of the 30K family (21, 54). The secondary structure of the members of the 30K family revealed that all MPs share a similar core structure (55), and the MPs of at least nine different genera are functionally exchangeable in the same viral system for local and systemic transport (56–58), permitting the possible extension of the proposed TMV MP topology to the other members of the 30K family. This topology should drive future investigations in search for host factors involved in plant viral transport.

ACKNOWLEDGMENTS

We thank Jari P. T. Valkonen for providing the pRT-YN-ER and pRT-YC-ER plasmids and S. Chapman for providing the infectious TMV plasmid.

This work was supported by grants BFU2009-08401 and BFU2012-39482 (to I.M.) and BIO2011-25018 (to V.P.) from the Spanish MINECO. A.P. is the recipient of a JAE predoc position (CSIC).

REFERENCES

1. **Verchot J.** 2011. Wrapping membranes around plant virus infection. Curr. Opin. Virol. **1:**388–395. http://dx.doi.org/10.1016/j.coviro.2011.09.009.
2. **Citovsky V, Wong ML, Shaw AL, Prasad BV, Zambryski P.** 1992. Visualization and characterization of tobacco mosaic virus movement protein binding to single-stranded nucleic acids. Plant Cell **4:**397–411. http://dx.doi.org/10.1105/tpc.4.4.397.
3. **Akiyama Y, Kamitani S, Kusukawa N, Ito K.** 1992. In vitro catalysis of oxidative folding of disulfide-bonded proteins by the *Escherichia coli dsbA* (*ppfA*) gene product. J. Biol. Chem. **267:**22440–22445.
4. **Crawford KM, Zambryski PC.** 2001. Non-targeted and targeted protein

movement through plasmodesmata in leaves in different developmental and physiological states. Plant Physiol. **125:**1802–1812. http://dx.doi.org/10.1104/pp.125.4.1802.
5. **Waigmann E, Lucas WJ, Citovsky V, Zambryski P.** 1994. Direct functional assay for tobacco mosaic virus cell-to-cell movement protein and identification of a domain involved in increasing plasmodesmal permeability. Proc. Natl. Acad. Sci. U. S. A. **91:**1433–1437. http://dx.doi.org/10.1073/pnas.91.4.1433.
6. **Wolf S, Deom CM, Beachy RN, Lucas WJ.** 1989. Movement protein of tobacco mosaic virus modifies plasmodesmatal size exclusion limit. Science **246:**377–379. http://dx.doi.org/10.1126/science.246.4928.377.
7. **Oparka KJ, Prior DA, Santa Cruz S, Padgett HS, Beachy RN.** 1997. Gating of epidermal plasmodesmata is restricted to the leading edge of expanding infection sites of tobacco mosaic virus (TMV). Plant J. **12:**781–789. http://dx.doi.org/10.1046/j.1365-313X.1997.12040781.x.
8. **Niehl A, Pena EJ, Amari K, Heinlein M.** 2013. Microtubules in viral replication and transport. Plant J. **75:**290–308. http://dx.doi.org/10.1111/tpj.12134.
9. **Boyko V, Hu Q, Seemanpillai M, Ashby J, Heinlein M.** 2007. Validation of microtubule-associated Tobacco mosaic virus RNA movement and involvement of microtubule-aligned particle trafficking. Plant J. **51:**589–603. http://dx.doi.org/10.1111/j.1365-313X.2007.03163.x.
10. **Sambade A, Brandner K, Hofmann C, Seemanpillai M, Mutterer J, Heinlein M.** 2008. Transport of TMV movement protein particles associated with the targeting of RNA to plasmodesmata. Traffic **9:**2073–2088. http://dx.doi.org/10.1111/j.1600-0854.2008.00824.x.
11. **Reichel C, Beachy RN.** 1998. Tobacco mosaic virus infection induces severe morphological changes of the endoplasmic reticulum. Proc. Natl. Acad. Sci. U. S. A. **95:**11169–11174. http://dx.doi.org/10.1073/pnas.95.19.11169.
12. **Beachy RN, Heinlein M.** 2000. Role of P30 in replication and spread of TMV. Traffic **1:**540–544. http://dx.doi.org/10.1034/j.1600-0854.2000.010703.x.
13. **Mas P, Beachy RN.** 1999. Replication of tobacco mosaic virus on endoplasmic reticulum and role of the cytoskeleton and virus movement protein in intracellular distribution of viral RNA. J. Cell Biol. **147:**945–958. http://dx.doi.org/10.1083/jcb.147.5.945.
14. **Heinlein M, Padgett HS, Gens JS, Pickard BG, Casper SJ, Epel BL, Beachy RN.** 1998. Changing patterns of localization of the tobacco mosaic virus movement protein and replicase to the endoplasmic reticulum and microtubules during infection. Plant Cell **10:**1107–1120. http://dx.doi.org/10.1105/tpc.10.7.1107.
15. **Brill LM, Nunn RS, Kahn TW, Yeager M, Beachy RN.** 2000. Recombinant tobacco mosaic virus movement protein is an RNA-binding, alpha-helical membrane protein. Proc. Natl. Acad. Sci. U. S. A. **97:**7112–7117. http://dx.doi.org/10.1073/pnas.130187897.
16. **Fujiki M, Kawakami S, Kim RW, Beachy RN.** 2006. Domains of tobacco mosaic virus movement protein essential for its membrane association. J. Gen. Virol. **87:**2699–2707. http://dx.doi.org/10.1099/vir.0.81936-0.
17. **Curin M, Ojangu EL, Trutnyeva K, Ilau B, Truve E, Waigmann E.** 2007. MPB2C, a microtubule-associated plant factor, is required for microtubular accumulation of tobacco mosaic virus movement protein in plants. Plant Physiol. **143:**801–811. http://dx.doi.org/10.1104/pp.106.091488.
18. **Shimizu T, Yoshii A, Sakurai K, Hamada K, Yamaji Y, Suzuki M, Namba S, Hibi T.** 2009. Identification of a novel tobacco DnaJ-like protein that interacts with the movement protein of tobacco mosaic virus. Arch. Virol. **154:**959–967. http://dx.doi.org/10.1007/s00705-009-0397-6.
19. **Chen MH, Sheng J, Hind G, Handa AK, Citovsky V.** 2000. Interaction between the tobacco mosaic virus movement protein and host cell pectin methylesterases is required for viral cell-to-cell movement. EMBO J. **19:**913–920. http://dx.doi.org/10.1093/emboj/19.5.913.
20. **Canto T, Palukaitis P.** 2002. Novel N gene-associated, temperature-independent resistance to the movement of tobacco mosaic virus vectors neutralized by a cucumber mosaic virus RNA1 transgene. J. Virol. **76:**12908–12916. http://dx.doi.org/10.1128/JVI.76.24.12908-12916.2002.
21. **Martinez-Gil L, Sanchez-Navarro JA, Cruz A, Pallas V, Perez-Gil J, Mingarro I.** 2009. Plant virus cell-to-cell movement is not dependent on the transmembrane disposition of its movement protein. J. Virol. **83:**5535–5543. http://dx.doi.org/10.1128/JVI.00393-09.
22. **Hessa T, Kim H, Bihlmaier K, Lundin C, Boekel J, Andersson H, Nilsson I, White SH, von Heijne G.** 2005. Recognition of transmembrane helices by the endoplasmic reticulum translocon. Nature **433:**377–381. http://dx.doi.org/10.1038/nature03216.
23. **Martinez-Gil L, Perez-Gil J, Mingarro I.** 2008. The surfactant peptide KL4 sequence is inserted with a transmembrane orientation into the endoplasmic reticulum membrane. Biophys. J. **95:**L36–38. http://dx.doi.org/10.1529/biophysj.108.138602.
24. **Herranz MC, Sanchez-Navarro JA, Sauri A, Mingarro I, Pallas V.** 2005. Mutational analysis of the RNA-binding domain of the Prunus necrotic ringspot virus (PNRSV) movement protein reveals its requirement for cell-to-cell movement. Virology **339:**31–41. http://dx.doi.org/10.1016/j.virol.2005.05.020.
25. **Zamyatnin AA, Jr, Solovyev AG, Bozhkov PV, Valkonen JP, Morozov SY, Savenkov EI.** 2006. Assessment of the integral membrane protein topology in living cells. Plant J. **46:**145–154. http://dx.doi.org/10.1111/j.1365-313X.2006.02674.x.
26. **Aparicio F, Sanchez-Navarro JA, Pallas V.** 2006. In vitro and in vivo mapping of the Prunus necrotic ringspot virus coat protein C-terminal dimerization domain by bimolecular fluorescence complementation. J. Gen. Virol. **87:**1745–1750. http://dx.doi.org/10.1099/vir.0.81696-0.
27. **Peremyslov VV, Pan YW, Dolja VV.** 2004. Movement protein of a closterovirus is a type III integral transmembrane protein localized to the endoplasmic reticulum. J. Virol. **78:**3704–3709. http://dx.doi.org/10.1128/JVI.78.7.3704-3709.2004.
28. **Saaf A, Wallin E, von Heijne G.** 1998. Stop-transfer function of pseudo-random amino acid segments during translocation across prokaryotic and eukaryotic membranes. Eur. J. Biochem. **251:**821–829. http://dx.doi.org/10.1046/j.1432-1327.1998.2510821.x.
29. **Martinez-Gil L, Sauri A, Vilar M, Pallas V, Mingarro I.** 2007. Membrane insertion and topology of the p7B movement protein of Melon Necrotic Spot Virus (MNSV). Virology **367:**348–357. http://dx.doi.org/10.1016/j.virol.2007.06.006.
30. **Hedin LE, Ojemalm K, Bernsel A, Hennerdal A, Illergard K, Enquist K, Kauko A, Cristobal S, von Heijne G, Lerch-Bader M, Nilsson I, Elofsson A.** 2010. Membrane insertion of marginally hydrophobic transmembrane helices depends on sequence context. J. Mol. Biol. **396:**221–229. http://dx.doi.org/10.1016/j.jmb.2009.11.036.
31. **Tamborero S, Vilar M, Martinez-Gil L, Johnson AE, Mingarro I.** 2011. Membrane insertion and topology of the translocating chain-associating membrane protein (TRAM). J. Mol. Biol. **406:**571–582. http://dx.doi.org/10.1016/j.jmb.2011.01.009.
32. **Ojemalm K, Halling KK, Nilsson I, von Heijne G.** 2012. Orientational preferences of neighboring helices can drive ER insertion of a marginally hydrophobic transmembrane helix. Mol. Cell **45:**529–540. http://dx.doi.org/10.1016/j.molcel.2011.12.024.
33. **Bano-Polo M, Martinez-Gil L, Wallner B, Nieva JL, Elofsson A, Mingarro I.** 2013. Charge pair interactions in transmembrane helices and turn propensity of the connecting sequence promote helical hairpin insertion. J. Mol. Biol. **425:**830–840. http://dx.doi.org/10.1016/j.jmb.2012.12.001.
34. **Bordier C.** 1981. Phase separation of integral membrane proteins in Triton X-114 solution. J. Biol. Chem. **256:**1604–1607.
35. **Kerppola TK.** 2008. Bimolecular fluorescence complementation (BiFC) analysis as a probe of protein interactions in living cells. Annu. Rev. Biophys. **37:**465–487. http://dx.doi.org/10.1146/annurev.biophys.37.032807.125842.
36. **Gafvelin G, Sakaguchi M, Andersson H, von Heijne G.** 1997. Topological rules for membrane protein assembly in eukaryotic cells. J. Biol. Chem. **272:**6119–6127. http://dx.doi.org/10.1074/jbc.272.10.6119.
37. **Goder V, Spiess M.** 2003. Molecular mechanism of signal sequence orientation in the endoplasmic reticulum. EMBO J. **22:**3645–3653. http://dx.doi.org/10.1093/emboj/cdg361.
38. **Sauri A, Tamborero S, Martinez-Gil L, Johnson AE, Mingarro I.** 2009. Viral membrane protein topology is dictated by multiple determinants in its sequence. J. Mol. Biol. **387:**113–128. http://dx.doi.org/10.1016/j.jmb.2009.01.063.
39. **Hessa T, Meindl-Beinker NM, Bernsel A, Kim H, Sato Y, Lerch-Bader M, Nilsson I, White SH, von Heijne G.** 2007. Molecular code for transmembrane-helix recognition by the Sec61 translocon. Nature **450:**1026–1030. http://dx.doi.org/10.1038/nature06387.
40. **Netherton C, Moffat K, Brooks E, Wileman T.** 2007. A guide to viral inclusions, membrane rearrangements, factories, and viroplasm produced during virus replication. Adv. Virus Res. **70:**101–182. http://dx.doi.org/10.1016/S0065-3527(07)70004-0.
41. **Hwang YT, McCartney AW, Gidda SK, Mullen RT.** 2008. Localization of the carnation Italian ringspot virus replication protein p36 to the mitochondrial outer membrane is mediated by an internal targeting signal and

the TOM complex. BMC Cell Biol. **9:**54. http://dx.doi.org/10.1186/1471-2121-9-54.
42. **Epel BL.** 2009. Plant viruses spread by diffusion on ER-associated movement-protein-rafts through plasmodesmata gated by viral induced host beta-1,3-glucanases. Semin. Cell Dev. Biol. **20:**1074–1081. http://dx.doi.org/10.1016/j.semcdb.2009.05.010.
43. **Vilar M, Sauri A, Monne M, Marcos JF, von Heijne G, Perez-Paya E, Mingarro I.** 2002. Insertion and topology of a plant viral movement protein in the endoplasmic reticulum membrane. J. Biol. Chem. **277:**23447–23452. http://dx.doi.org/10.1074/jbc.M202935200.
44. **Martinez-Gil L, Johnson AE, Mingarro I.** 2010. Membrane insertion and biogenesis of the Turnip crinkle virus p9 movement protein. J. Virol. **84:**5520–5527. http://dx.doi.org/10.1128/JVI.00125-10.
45. **Genoves A, Pallas V, Navarro JA.** 2011. Contribution of topology determinants of a viral movement protein to its membrane association, intracellular traffic, and viral cell-to-cell movement. J. Virol. **85:**7797–7809. http://dx.doi.org/10.1128/JVI.02465-10.
46. **Tyulkina LG, Karger EM, Sheveleva AA, Atabekov JG.** 2010. Binding of monoclonal antibodies to the movement protein (MP) of Tobacco mosaic virus: influence of subcellular MP localization and phosphorylation. J. Gen. Virol. **91:**1621–1628. http://dx.doi.org/10.1099/vir.0.018002-0.
47. **Boyko V, Ferralli J, Ashby J, Schellenbaum P, Heinlein M.** 2000. Function of microtubules in intercellular transport of plant virus RNA. Nat. Cell Biol. **2:**826–832. http://dx.doi.org/10.1038/35041072.
48. **Ashby J, Boutant E, Seemanpillai M, Groner A, Sambade A, Ritzenthaler C, Heinlein M.** 2006. Tobacco mosaic virus movement protein functions as a structural microtubule-associated protein. J. Virol. **80:**8329–8344. http://dx.doi.org/10.1128/JVI.00540-06.
49. **Citovsky V, Knorr D, Schuster G, Zambryski P.** 1990. The P30 movement protein of tobacco mosaic virus is a single-strand nucleic acid binding protein. Cell **60:**637–647. http://dx.doi.org/10.1016/0092-8674(90)90667-4.
50. **Strasser M, Pfitzner AJ.** 2007. The double-resistance-breaking Tomato mosaic virus strain ToMV1-2 contains two independent single resistance-breaking domains. Arch. Virol. **152:**903–914. http://dx.doi.org/10.1007/s00705-006-0915-8.
51. **Denecke J, Carlsson LE, Vidal S, Hoglund AS, Ek B, van Zeijl MJ, Sinjorgo KM, Palva ET.** 1995. The tobacco homolog of mammalian calreticulin is present in protein complexes in vivo. Plant Cell **7:**391–406. http://dx.doi.org/10.1105/tpc.7.4.391.
52. **Borisjuk N, Sitailo L, Adler K, Malysheva L, Tewes A, Borisjuk L, Manteuffel R.** 1998. Calreticulin expression in plant cells: developmental regulation, tissue specificity and intracellular distribution. Planta **206:**504–514. http://dx.doi.org/10.1007/s004250050427.
53. **Jia XY, He LH, Jing RL, Li RZ.** 2009. Calreticulin: conserved protein and diverse functions in plants. Physiol. Plant **136:**127–138. http://dx.doi.org/10.1111/j.1399-3054.2009.01223.x.
54. **Laporte C, Vetter G, Loudes AM, Robinson DG, Hillmer S, Stussi-Garaud C, Ritzenthaler C.** 2003. Involvement of the secretory pathway and the cytoskeleton in intracellular targeting and tubule assembly of Grapevine fanleaf virus movement protein in tobacco BY-2 cells. Plant Cell **15:**2058–2075. http://dx.doi.org/10.1105/tpc.013896.
55. **Melcher U.** 2000. The '30K' superfamily of viral movement proteins. J. Gen. Virol. **81:**257–266.
56. **Sanchez-Navarro JA, Carmen Herranz M, Pallas V.** 2006. Cell-to-cell movement of alfalfa mosaic virus can be mediated by the movement proteins of ilar-, bromo-, cucumo-, tobamo- and comoviruses and does not require virion formation. Virology **346:**66–73. http://dx.doi.org/10.1016/j.virol.2005.10.024.
57. **Sanchez-Navarro J, Fajardo T, Zicca S, Pallas V, Stavolone L.** 2010. Caulimoviridae tubule-guided transport is dictated by movement protein properties. J. Virol. **84:**4109–4112. http://dx.doi.org/10.1128/JVI.02543-09.
58. **Fajardo TV, Peiro A, Pallas V, Sanchez-Navarro J.** 2013. Systemic transport of Alfalfa mosaic virus can be mediated by the movement proteins of several viruses assigned to five genera of the 30K family. J. Gen. Virol. **94:**677–681. http://dx.doi.org/10.1099/vir.0.048793-0.